Mutation-induced Blocker Permeability and Multiion Block of the CFTR Chloride Channel Pore

Xiandi Gong and Paul Linsdell

Department of Physiology and Biophysics, Dalhousie University, Halifax, Nova Scotia B3H 4H7, Canada

ABSTRACT Chloride permeation through the cystic fibrosis transmembrane conductance regulator (CFTR) Cl^- channel is blocked by a broad range of anions that bind tightly within the pore. Here we show that the divalent anion $Pt(NO_2)_4^{2-}$ acts as an impermeant voltage-dependent blocker of the CFTR pore when added to the intracellular face of excised membrane patches. Block was of modest affinity (apparent K_d 556 μM), kinetically fast, and weakened by extracellular Cl^- ions. A mutation in the pore region that alters anion selectivity, F337A, but not another mutation at the same site that has no effect on selectivity (F337Y), had a complex effect on channel block by intracellular $Pt(NO_2)_4^{2-}$ ions. Relative to wild-type, block of F337A-CFTR was weakened at depolarized voltages but strengthened at hyperpolarized voltages. Current in the presence of $Pt(NO_2)_4^{2-}$ increased at very negative voltages in F337A but not wild-type or F337Y, apparently due to relief of block by permeation of $Pt(NO_2)_4^{2-}$ ions to the extracellular solution. This "punchthrough" was prevented by extracellular Cl^- ions, reminiscent of a "lock-in" effect. Relief of block in F337A by $Pt(NO_2)_4^{2-}$ permeation was only observed for blocker concentrations above 300 μM; as a result, block at very negative voltages showed an anomalous concentration dependence, with an increase in blocker concentration causing a significant weakening of block and an increase in Cl^- current. We interpret this effect as reflecting concentration-dependent permeability of $Pt(NO_2)_4^{2-}$ in F337A, an apparent manifestation of an anomalous mole fraction effect. We suggest that the F337A mutation allows intracellular $Pt(NO_2)_4^{2-}$ to enter deeply into the CFTR pore where it interacts with multiple binding sites, and that simultaneous binding of multiple $Pt(NO_2)_4^{2-}$ ions within the pore promotes their permeation to the extracellular solution.

KEY WORDS: anion channel • ion permeation • multiion pore • voltage-dependent block • cystic fibrosis

INTRODUCTION

Ion channels allow the selective movement of ions across cell membranes at very high rates. This process is best understood in highly selective K^+ channel pores that can now be observed at atomic resolution (Doyle et al., 1998; Zhou et al., 2001). These pores contain several K^+ ion binding sites, and multiple K^+ ions move through the pore in a concerted fashion (Bernèche and Roux, 2001; Morais-Cabral et al., 2001). The permeation mechanism so unequivocally proven by the K^+ channel X-ray crystal structure (Morais-Cabral et al., 2001; Zhou et al., 2001), that ions bind to specific sites within the pore, and unbinding and rapid conduction then results from electrostatic repulsion between ions bound simultaneously within the pore, had long been suggested based on functional evidence from electrophysiological experimentation (Hodgkin and Keynes, 1955; Neyton and Miller, 1988a,b; Jiang and MacKinnon, 2000). A similar mechanism probably also accounts for Ca^{2+} selectivity and permeation in voltage gated Ca^{2+} channels (Sather and McCleskey, 2003).

Recently, crystal structures of ClC Cl^- channels have been presented (Dutzler et al., 2002, 2003). In a fascinating parallel with the K^+ channels described above, Cl^- ions are observed bound to three sites in the ClC channel pore, and these binding sites are as close together as 4 Å (Dutzler et al., 2003). Again as with K^+ channels, this agrees with prior functional evidence that ClC channels have multiion pores that are capable of holding more than one anion simultaneously (Pusch et al., 1995; Fahlke et al., 1997; Rychkov et al., 1998; Winters and Andreoli, 2002; Hebeisen et al., 2003). This might suggest a similar Cl^- permeation mechanism in these channels to that now accepted for K^+ channel permeation (Dutzler et al., 2003). Other, structurally unrelated classes of Cl^- channels also show biophysical properties of multiion pore behavior (Bormann et al., 1987; Halm and Frizzell, 1992; Tabcharani et al., 1993; Dawson et al., 1999; Qu and Hartzell, 2000).

The cystic fibrosis transmembrane conductance regulator (CFTR) is a phosphorylation-regulated, ATP-

Address correspondence to Paul Linsdell, Department of Physiology and Biophysics, Dalhousie University, Sir Charles Tupper Medical Building, Halifax, Nova Scotia B3H 4H7, Canada. Fax: (902) 494-1685; email: Paul.Lindsell@dal.ca

Abbreviations used in this paper: BHK, baby hamster kidney; CHO, Chinese hamster ovary; PPi, pyrophosphate; TES, *N*-tris[hydroxymethyl]methyl-2-aminoethanesulfonate; TM6, sixth transmembrane region.

J. Gen. Physiol. © The Rockefeller University Press • 0022-1295/2003/12/673/15 $8.00
Volume 122 December 2003 673–687
http://www.jgp.org/cgi/doi/10.1085/jgp.200308889

dependent epithelial Cl^- channel (Sheppard and Welsh, 1999). As with most Cl^- channels, CFTR is weakly selective between different anions, although it selects strongly for anions over cations (Dawson et al., 1999). Its anion permeability sequence is similar to a classical Hofmeister or lyotropic sequence, with anions that are more easily dehydrated (lyotropes) tending to show a higher permeability than anions that retain their waters of hydration more strongly (kosmotropes) (Dawson et al., 1999). Lyotropic anions also bind relatively tightly within the CFTR Cl^- channel pore, and as such they act as effective open-channel blockers of Cl^- permeation (Tabcharani et al., 1993; Smith et al., 1999; Linsdell, 2001a; Linsdell and Gong, 2002). This mechanism of action is similar to that of a broad range of organic anions that act as open channel blockers of CFTR (Hwang and Sheppard, 1999; Linsdell, 2001b). These large blockers tend to act preferentially or exclusively from the intracellular side of the membrane, implying a structural asymmetry in the pore (Linsdell and Hanrahan, 1996a; Hwang and Sheppard, 1999; Linsdell, 2001b; Zhou et al., 2002).

Open-channel blockers have previously been used to reveal multiion pore behavior in the CFTR channel pore (Tabcharani et al., 1993; Zhou et al., 2002; Gong and Linsdell, 2003a). Most recently, we have used the highly permeant monovalent pseudohalide anion $Au(CN)_2^-$ as a functional probe of anion binding sites in the CFTR pore (Gong et al., 2002a; Gong and Linsdell, 2003a,b). Here we characterize the blocking effects of divalent pseudohalide anions on CFTR, and provide evidence that binding of multiple anions within the CFTR pore promotes their permeation through the channel. We suggest that such a multiion mechanism may be part of the normal Cl^- ion permeation process.

MATERIALS AND METHODS

Experiments were performed on two mammalian cell lines, baby hamster kidney (BHK) and Chinese hamster ovary (CHO) cells. BHK cells used for macroscopic current recording were transiently transfected with wild-type or mutant forms of human CFTR in the pIRES2-EGFP vector (CLONTECH) as described previously (Gong et al., 2002a). Briefly, plasmid DNA was precomplexed with Plus reagent (Life Technologies) for 15 min, followed by Lipofectamine (Life Technologies) for a further 15 min. Complexed DNA was then diluted in supplement-free medium to a final concentration of 0.5 μg ml^{-1} and added to the cells. After 5 h at 37°C and 5% CO_2, the medium was completely replaced with normal medium containing 5% fetal bovine serum. Transiently transfected cells could be identified by fluorescence microscopy within 24 h and were used for patch clamp recording 1–4 d after transfection. CHO cells used for single-channel recording were stably transfected with wild-type human CFTR (Tabcharani et al., 1991). In most cases, recordings were made using the excised, inside-out configuration of the patch clamp technique, as described in detail previously (Linsdell and Gong, 2002). Briefly, CFTR channels were activated after patch excision by exposure to 15–60 nM protein kinase A catalytic subunit (PKA) plus 1 mM MgATP. For blocker experiments, both the extracellular (pipette) and intracellular (bath) solutions contained (mM): 150 NaCl, 10 *N*-tris[hydroxymethyl]methyl-2-aminoethanesulfonate (TES), 2 $MgCl_2$, except where extracellular [Cl^-] was reduced to 4 mM by replacement of 150 mM NaCl by 150 mM Na gluconate, $NaNO_3$, or $NaClO_4$. For all macroscopic current block experiments except in Fig. 2 A, CFTR channels were "locked" in the open state by addition of 2 mM sodium pyrophosphate (PPi) to the intracellular solution after attainment of full PKA-stimulated current amplitude (Gunderson and Kopito, 1994) as described previously (Gong et al., 2002a; Linsdell and Gong, 2002; Gong and Linsdell, 2003a,b). To estimate $Pt(NO_2)_4^{2-}$ permeability, the intracellular solution contained (mM): 100 $K_2Pt(NO_2)_4$, 10 TES, 2 $MgCl_2$, and the extracellular solution was (mM): 150 KCl, 10 TES, 2 $MgCl_2$. In some cases (Fig. 3 C), outside-out patches were employed; here both the intracellular (pipette) and extracellular (bath) solutions contained (mM): 150 NaCl, 10 TES, 2 $MgCl_2$, and CFTR channel activity was maintained by inclusion of 50 nM PKA plus 1 mM MgATP in the pipette solution. Putative blockers ($K_2Pt(NO_2)_4$, K_2PtCl_4, $K_3Fe(CN)_6$, $K_3Co(CN)_6$) were added to the bath solution from stocks made up in normal experimental solutions. All solutions were adjusted to pH 7.4 using NaOH or KOH as appropriate. Given voltages have been corrected for calculated or measured liquid junction potentials. All chemicals were from Sigma-Aldrich except PKA (Promega) and $K_2Pt(NO_2)_4$, K_2PtCl_4, and $K_3Co(CN)_6$ (Strem Chemicals).

Current traces were filtered at 50 Hz (for single-channel currents) or 100 Hz (for macroscopic currents) using an eight-pole Bessel filter, digitized at 250 Hz to 1 kHz, and analyzed using pCLAMP8 software (Axon Instruments, Inc.). Macroscopic current-voltage relationships were constructed using depolarizing ramp protocols (Linsdell and Hanrahan, 1996a; Linsdell and Gong, 2002) or conventional voltage steps. Except where indicated, background (leak) currents recorded before addition of PKA were subtracted digitally, leaving uncontaminated CFTR currents (Linsdell and Hanrahan, 1996a, 1998). The macroscopic current reversal potential (Fig. 4) was estimated by fitting a polynomial function to the leak-subtracted current-voltage relationship.

Blocker concentration-inhibition relationships (Fig. 1, B and D) were fitted by an equation of the form:

$$\text{Fractional unblocked current} = 1/[1 + (B/K_d)^{n_H}], \quad (1)$$

where B is the blocker concentration, K_d the apparent blocker dissociation constant, and n_H the slope factor or Hill coefficient.

The relationship between the fractional unblocked current and membrane voltage was routinely fitted by the simplest version of the Woodhull (1973) model of voltage-dependent block:

$$I/I_0 = K_d(V)/\{K_d(V) + [B]\}, \quad (2)$$

where I is the current in the presence of blocker, I_0 is the control, unblocked current, and $K_d(V)$ is the voltage dependent dissociation constant, the voltage dependence of which is given by:

$$K_d(V) = K_d(0)\exp(-z\delta VF/RT), \quad (3)$$

where $z\delta$ is the effective valence of the blocking ion (actual valence multiplied by the fraction of the transmembrane electric field apparently experienced during the blocking reaction), and F, R, and T have their normal thermodynamic meanings.

All other methodological details were as described in detail recently (Linsdell and Gong, 2002; Gong et al., 2002a,b). Experiments were performed at room temperature, 21–24°C. Mean values are given as mean ± SEM. Statistical comparisons between groups were performed using a two-tailed *t* test, with $P < 0.05$ being considered statistically significant.

RESULTS

Block of CFTR by Divalent Pseudohalide Anions

The monovalent pseudohalide anion $Au(CN)_2^-$ is a potent blocker of the CFTR Cl^- channel when added to the intracellular side of the membrane (Linsdell and Gong, 2002). We investigated the inhibitory effects of divalent and trivalent pseudohalide anions using a similar approach (Fig. 1). Addition of $Pt(NO_2)_4^{2-}$ or $PtCl_4^{2-}$ to the intracellular solution caused a voltage-dependent block of macroscopic CFTR currents in inside-out membrane patches (Fig. 1 A) after channel "locking open" with PPi (see below). In contrast, $Fe(CN)_6^{3-}$ and $Co(CN)_6^{3-}$ had no apparent effect on CFTR currents at intracellular concentrations up to 1 mM (Fig. 1 A). Fig. 1 also shows the concentration and voltage dependence of inhibition by $Pt(NO_2)_4^{2-}$ (Fig. 1, B and C) and $PtCl_4^{2-}$ (Fig. 1, D and E). The straight line fits to Fig. 1, C and E suggest a K_d at 0 mV of 556 μM for $Pt(NO_2)_4^{2-}$ and 969 μM for $PtCl_4^{2-}$, and an effective valence, $z\delta$, of −0.432 for $Pt(NO_2)_4^{2-}$ and −0.167 for $PtCl_4^{2-}$ (see MATERIALS AND METHODS). Subsequent experiments focused on the more potent of these blockers, $Pt(NO_2)_4^{2-}$.

As previously described for $Au(CN)_2^-$ (Linsdell and Gong, 2002), the apparent affinity of block by $Pt(NO_2)_4^{2-}$ was decreased by treatment of the channels with PPi (Fig. 2 A), although this effect was far less striking than for $Au(CN)_2^-$ (Linsdell and Gong, 2002). Under the conditions shown in Fig. 2 A, the mean $K_d(0)$, estimated by fitting to Eq. 2, was increased from 137 ± 12 μM ($n = 5$) in the absence of PPi to 482 ± 62 μM ($n = 9$) after PPi-stimulation ($P < 0.05$). The effect of PPi on the inhibition of CFTR channels by intracellular $Au(CN)_2^-$ was shown previously to be due to alteration of channel gating by $Au(CN)_2^-$ (Linsdell and Gong, 2002). To obviate any similar effects of $Pt(NO_2)_4^{2-}$ on channel gating and to isolate effects on open CFTR channels, all experiments other than those shown in Figs. 2 A and 3 were performed on CFTR channels that

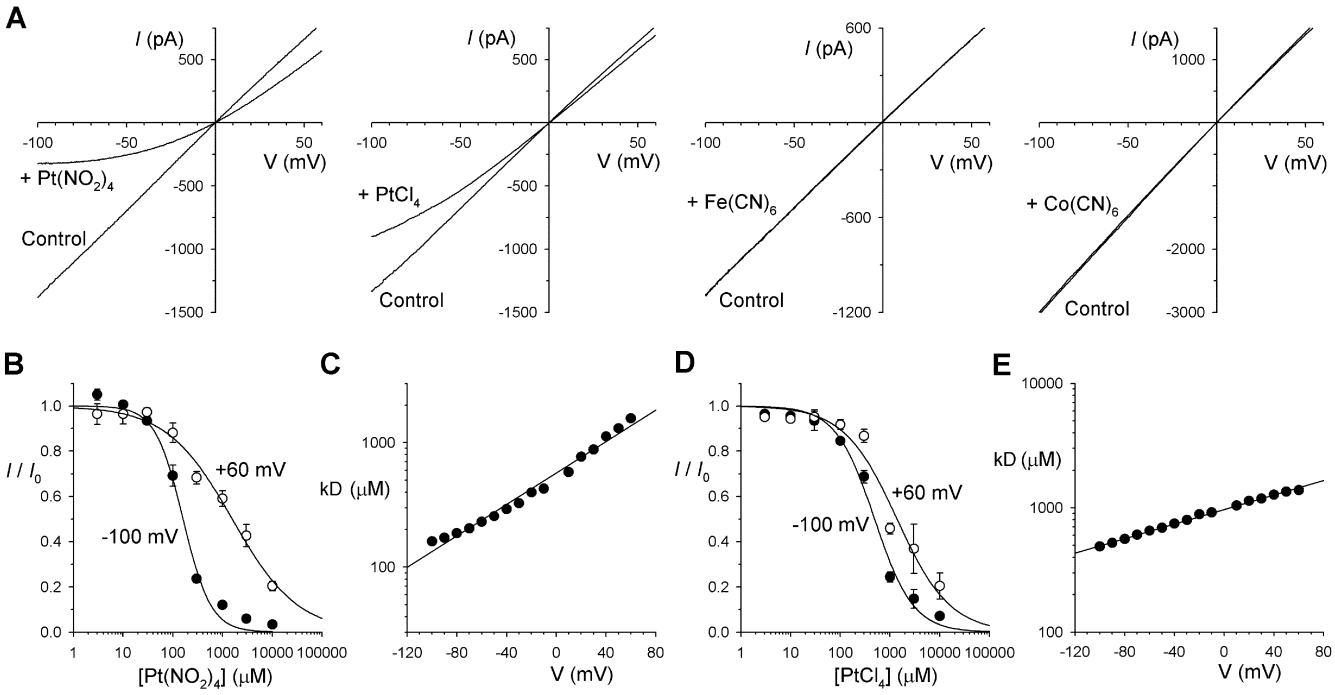

FIGURE 1. Intracellular divalent pseudohalide anions inhibit CFTR Cl^- currents. (A) Example leak-subtracted macroscopic CFTR currents in inside-out membrane patches, stimulated by PKA, ATP, and PPi, before (Control) and after addition of different pseudohalide anions (300 μM $Pt(NO_2)_4^{2-}$, 300 μM $PtCl_4^{2-}$, 1 mM $Fe(CN)_6^{3-}$, 1 mM $Co(CN)_6^{3-}$) to the intracellular solution. (B and D) Mean fraction of control current remaining (I/I_0) after addition of different concentrations of $Pt(NO_2)_4^{2-}$ (B) or $PtCl_4^{2-}$ (D) to the intracellular solution, at a membrane potential of −100 mV (●) or +60 mV (○). Mean of data from 3–9 patches, fitted by Eq. 1 with the following parameters: for $Pt(NO_2)_4^{2-}$, K_d 161 μM, and n_H 1.45 at −100 mV, and K_d 1,567 μM and n_H 0.71 at +60 mV; and for $PtCl_4^{2-}$, K_d 489 μM and n_H 1.12 at −100 mV, and K_d 1383 μM and n_H 0.82 at +60 mV. (C and E) Voltage dependence of K_d estimated from fits such as those shown in (B and D), for $Pt(NO_2)_4^{2-}$ (C) and $PtCl_4^{2-}$ (E). Straight line fits give K_ds at 0 mV of 556 μM for $Pt(NO_2)_4^{2-}$ (C) and 969 μM for $PtCl_4^{2-}$ (E), and $z\delta$ values of −0.432 for $Pt(NO_2)_4^{2-}$ and −0.167 for $PtCl_4^{2-}$.

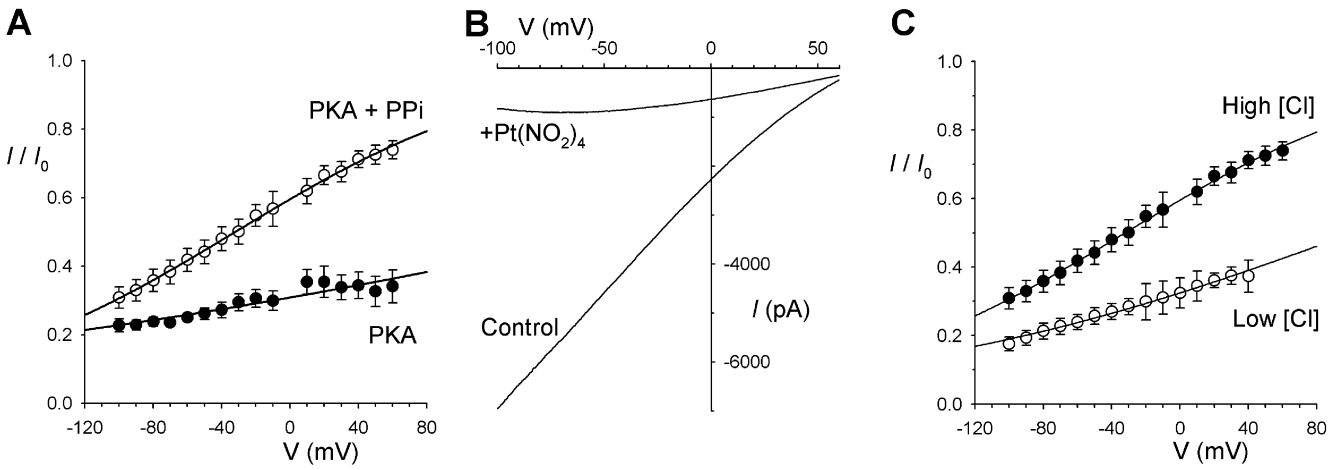

FIGURE 2. Pyrophosphate and Cl^- dependence of $Pt(NO_2)_4^{2-}$ block. (A) Mean fraction of control current remaining following addition of 300 μM $Pt(NO_2)_4^{2-}$ after full CFTR channel activation with PKA plus ATP (●) or following subsequent "locking open" with 2 mM PPi (○). Mean of data from 6–9 patches fitted by Eq. 2, with $K_d(0)$ = 134 μM and $z\delta$ = −0.105 without PPi (●) and $K_d(0)$ = 441 μM and $z\delta$ = −0.307 in the presence of PPi (○). (B) Example macroscopic CFTR current recorded with 4 mM extracellular Cl^-, before (Control) and after addition of 300 μM $Pt(NO_2)_4^{2-}$ to the intracellular solution. (C) Mean fraction of control current remaining after addition of 300 μM $Pt(NO_2)_4^{2-}$, at extracellular Cl^- concentrations of 154 mM (●) or 4 mM (○). Mean of data from 6–9 patches fitted by Eq. 2, with $K_d(0)$ = 441 μM and $z\delta$ = −0.307 with 154 mM Cl^- (●) and $K_d(0)$ = 144 μM and $z\delta$ = −0.184 with 4 mM Cl^- (○).

had been "locked open" using 2 mM PPi, as in previous studies (Gong and Linsdell, 2003a,b).

Reducing extracellular Cl^- concentration from 154 to 4 mM (by replacement with the impermeant anion gluconate) strengthened the block and decreased its voltage dependence (Fig. 2, B and C), again in common with previous studies using $Au(CN)_2^-$ (Gong and Linsdell, 2003a) and other open channel blockers (McDonough et al., 1994; Sheppard and Robinson, 1997; Linsdell and Hanrahan, 1999; Gong et al., 2002b; Zhou et al., 2002). With both high and low extracellular Cl^- concentrations, the voltage dependence of block was well described by a simple Woodhull model (Fig. 2 C). Fits to Eq. 2 such as those in Fig. 2 C indicate a $K_d(0)$ of 482 ± 62 μM (n = 9) with 154 mM Cl^- and 154 ± 13 μM (n = 9) with 4 mM Cl^- ($P < 0.0001$), and a $z\delta$ of −0.321 ± 0.011 (n = 9) with 154 mM Cl^- and –0.222 ± 0.029 (n = 9) with 4 mM Cl^- ($P < 0.01$). Similar, statistically significant effects of both PPi and changing the extracellular Cl^- concentration were observed for block by $PtCl_4^{2-}$ (unpublished data).

At the single-channel level, intracellular $Pt(NO_2)_4^{2-}$ caused a voltage-dependent decrease in CFTR unitary current amplitude (Fig. 3, A and B) that was of similar potency to the block of PPi-stimulated macroscopic currents (e.g., Fig. 1 A). For example, the fractional current remaining in the presence of 300 μM $Pt(NO_2)_4^{2-}$ at −80 mV was 0.358 ± 0.032 (n = 6) for macroscopic currents and 0.379 ± 0.009 (n = 5) for single-channel currents; and, at +50 mV, 0.725 ± 0.028 (n = 6) for macroscopic currents and 0.753 ± 0.031 (n = 5) for single-channel currents. In contrast, addition of extracellular $Pt(NO_2)_4^{2-}$ caused a weaker, less voltage-dependent reduction in unitary current amplitude of CFTR channels in outside-out membrane patches (Fig. 3, C and D). All of these results are consistent with $Pt(NO_2)_4^{2-}$ acting as an unremarkable open-channel blocker of the CFTR Cl^- channel.

Permeability of $Pt(NO_2)_4$

Previously, divalent pseudohalides including $Pt(NO_2)_4^{2-}$ have been described as being impermeant in the CFTR Cl^- channel (Smith and Dawson, 2001). We attempted to measure the permeability of $Pt(NO_2)_4^{2-}$ ions when present in the intracellular solution (Fig. 4). With 100 mM $Pt(NO_2)_4^{2-}$ plus 4 mM Cl^- in the intracellular solution, and 154 mM Cl^- in the extracellular solution, the current reversal potential was −95 ± 5 mV (n = 3) (Fig. 4 C), similar to the calculated Cl^- equilibrium potential of −93 mV, consistent with $Pt(NO_2)_4^{2-}$ being unable to carry current through the CFTR channel.

Block of CFTR Pore Mutants

Other CFTR open channel blocking anions have previously been suggested to interact with key residues in the pore-forming sixth transmembrane (TM6) region of the channel protein (McDonough et al., 1994; Walsh et al., 1999; Zhang et al., 2000; Gong et al., 2002a,b; Gupta and Linsdell, 2002; Gong and Linsdell, 2003b). We investigated the interaction of intracellular $Pt(NO_2)_4^{2-}$ with CFTR channels bearing mutations at each of five key TM6 residues: R334, K335, F337, T338, and S341 (Fig. 5). The I-V relationships of these mu-

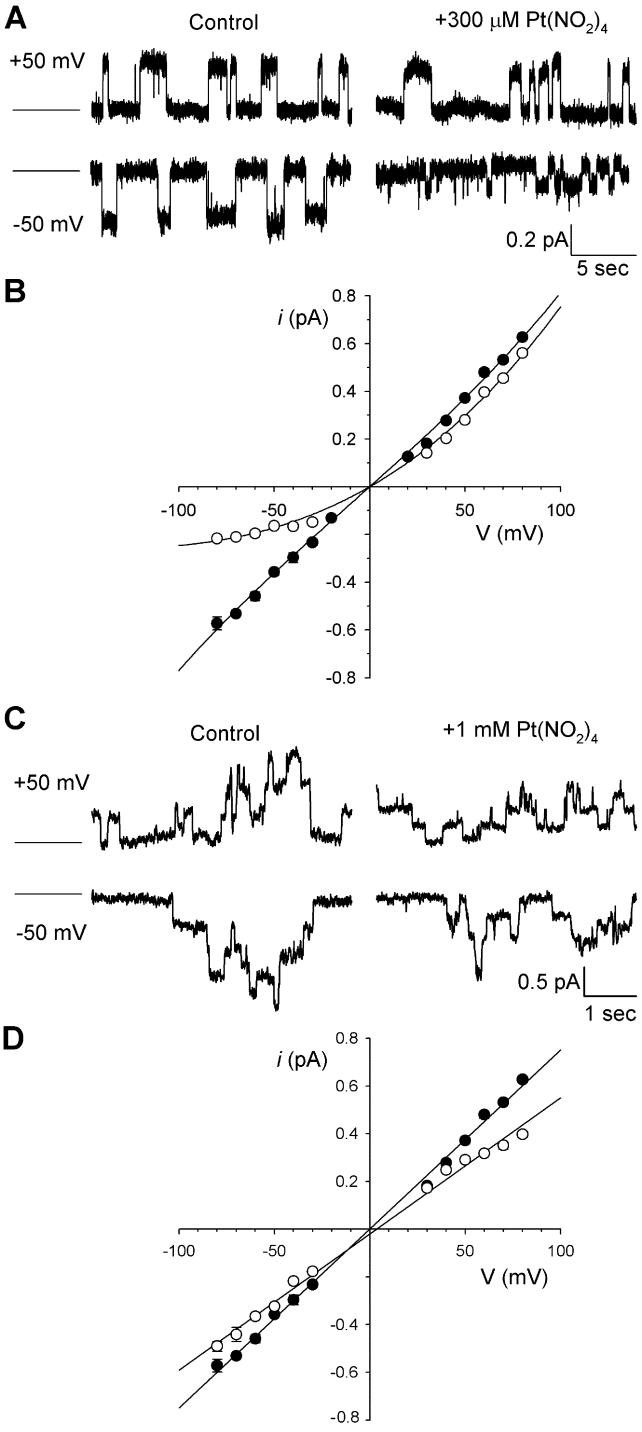

FIGURE 3. Effect of $Pt(NO_2)_4^{2-}$ on CFTR unitary currents recorded from membrane patches excised from CHO cells stably expressing wild-type CFTR in the absence of PPi. (A) Single-channel currents recorded from an inside-out patch at the membrane potentials indicated on the left, before (Control) and after addition of 300 μM $Pt(NO_2)_4^{2-}$ to the intracellular solution. The closed state current is indicated by the straight line to the far left in each case. (B) Mean unitary current-voltage relationships for the predominant, fully open state of the channel (Gunderson and Kopito, 1995) recorded from inside-out membrane patches under control conditions (●) and in the presence of 300 μM intracellular $Pt(NO_2)_4^{2-}$ (○). (C) Unitary currents recorded from an outside-out patch before (Control) and after addition of 1 mM $Pt(NO_2)_4^{2-}$ to the extracellular solution. (D) Mean unitary current-voltage relationships recorded from outside-out membrane patches under control conditions (●) and in the presence of 1 mM extracellular $Pt(NO_2)_4^{2-}$ (○). Mean of data from 3–10 patches in B and D.

tants showed varying degrees of inward rectification, as previously quantified by Gupta and Linsdell (2003). Block of R334C and S341A appeared somewhat weaker than for wild-type CFTR, whereas K335A and T338A showed a similar degree of block as wild-type (Fig. 5, A–C). In all four of these mutants, the voltage dependence of block still appeared well described by a simple Woodhull model (Fig. 5 B). In contrast, block of F337A was poorly described by the Woodhull model (Fig. 5 B), with block of this mutant appearing to be very much more voltage dependent at negative voltages than at positive voltages (Fig. 5 B). Although estimation of the blocking effects of $Pt(NO_2)_4^{2-}$ at 0 mV membrane potential suggested a slight but significant weakening of block in F337A compared with wild-type (Fig. 5 C), direct comparison of the blocking effects of 300 μM $Pt(NO_2)_4^{2-}$ on wild-type and F337A (Fig. 5 D) suggests that while block is weakened in this mutant at depolarized voltages, the block is actually stronger in F337A than in wild-type at strongly hyperpolarized voltages. Neither of these effects were observed in another F337 mutant, F337Y, which was blocked in an apparently similar manner as wild-type (Fig. 5, C and E).

The Interaction between $Pt(NO_2)_4$ and F337A-CFTR

Compared with the unremarkable block of wild-type CFTR by intracellular $Pt(NO_2)_4^{2-}$ (Figs. 1–3), block of F337A-CFTR appears complex. Block of this mutant appears to be strongly favored by negative membrane potentials (Fig. 5, A, B, and D). However, when we investigated the block at the most negative voltages that we were able to keep membrane patches (−150 mV) with a low extracellular Cl^- concentration (4 mM), we noticed an anomalous voltage-dependent increase in $Pt(NO_2)_4^{2-}$-blocked current in F337A but not in wild-type, F337Y or T338A (Fig. 6). Under these conditions, the strength of $Pt(NO_2)_4^{2-}$ block in wild-type, F337Y, and T338A increases with increasingly negative voltages, eventually leading to a negative slope of the current-voltage relationship in the presence of blocker (Fig. 6 B). However, in F337A, the current in the presence of blocker increases again at voltages more negative than around −80 mV, suggesting that as the membrane potential is made very negative blocking ions are swept from the pore and Cl^- is able more easily to permeate. This kind of behavior has been observed in cation selective channels (French and Wells, 1977; French and Shoukimas, 1985; Bähr-

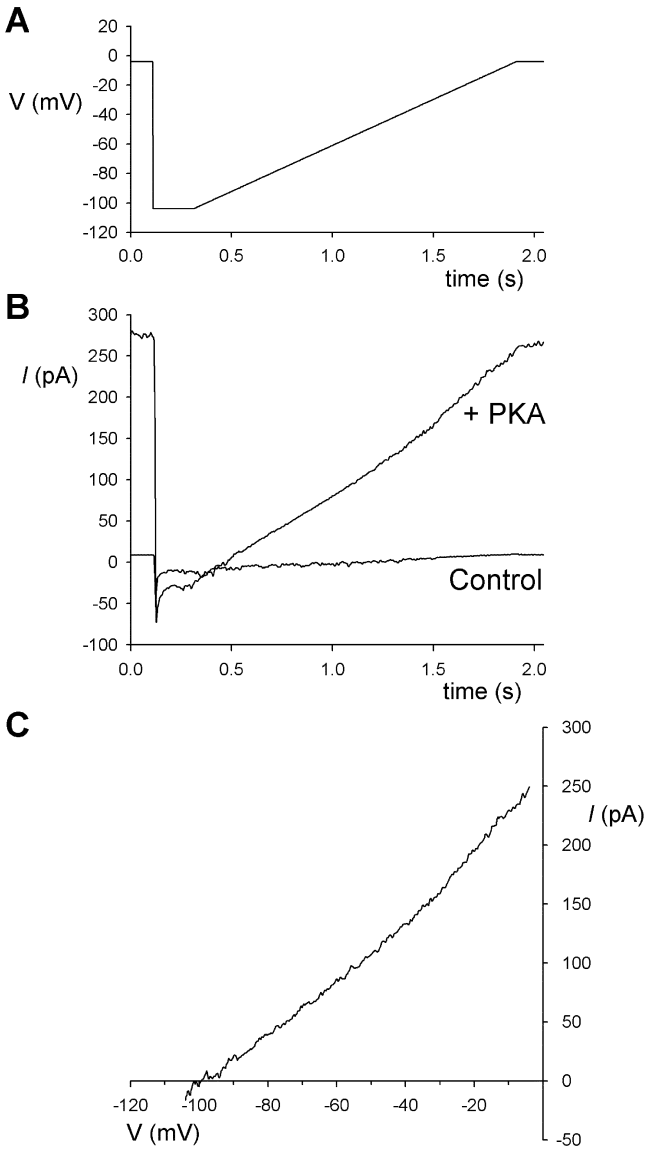

FIGURE 4. $Pt(NO_2)_4^{2-}$ is not measurably permeant in wild-type CFTR. (A) Voltage-ramp protocol used to measure $Pt(NO_2)_4^{2-}$ permeability. (B) Example raw unsubtracted macroscopic currents recorded with 100 mM $Pt(NO_2)_4^{2-}$ plus 4 mM Cl^- in the intracellular solution and 154 mM Cl^- in the extracellular solution, before (Control) and after CFTR channel stimulation with PKA in the presence of ATP. (C) Subtraction of the control current from the PKA-stimulated current in B allows isolation of the CFTR current and estimation of its reversal potential.

ing et al., 1997; Huang et al., 2000; Huang and Moczydlowski, 2001; Nimigean and Miller, 2002; Kerschbaum et al., 2003) and is most easily explained by blocker permeation through the channel. Thus, at very negative voltages, $Pt(NO_2)_4^{2-}$ ions can escape from the F337A channel pore, but apparently not from the pore of wild-type, F337Y or T338A, by passing through the channel and into the extracellular solution—a process previously termed "punchthrough" (Nimigean and Miller, 2002).

Interestingly, $Pt(NO_2)_4^{2-}$ punchthrough in F337A was observed at low (Fig. 6) but not high extracellular Cl^- concentrations (Fig. 7), suggesting that extracellular Cl^- ions can prevent $Pt(NO_2)_4^{2-}$ from passing through this mutant channel. Punchthrough was also apparently prevented by the highly permeant nitrate (NO^{3-}) ion in the extracellular solution (Fig. 7). However, when the lyotropic perchlorate (ClO_4^-) anion, which binds tightly in the CFTR pore (Linsdell, 2001a) but is only weakly permeant (Linsdell and Hanrahan, 1998), was present in the extracellular solution, punchthrough was still observed (Fig. 7).

Concentration-inhibition experiments with low extracellular Cl^- concentrations confirmed the multiple apparent effects of the F337A mutation on the apparent affinity of $Pt(NO_2)_4^{2-}$ block (Fig. 8). At relatively depolarized voltages (e.g., 0 mV; Fig. 8 C), $Pt(NO_2)_4^{2-}$ blocked wild-type more strongly than F337A (i.e., the concentration-inhibition curve for wild-type lies to the left); whereas at hyperpolarized voltages (e.g., −130 mV, Fig. 8 D), the mutant is more potently inhibited. However, these experiments also illustrate that the punchthrough mechanism that relieves block of F337A but not wild-type at strongly hyperpolarized voltages is dependent not only on voltage but also on the blocker concentration. This concentration dependence is shown more clearly in Fig. 9. As expected, increasing the concentration of blocker from 100 to 300 μM strengthened the block at positive voltages (Fig. 9 A). However, this increase in blocker concentration caused an anomalous weakening of block at very negative voltages (Fig. 9, A and B). Indeed, the degree of block seen with 300 μM $Pt(NO_2)_4^{2-}$ was significantly less than that with 100 μM at each voltage between −110 and −150 mV ($P < 0.05$ in each case). Increasing the concentration of $Pt(NO_2)_4^{2-}$ further, to 1 mM, strengthened the block at all voltages (Fig. 9 B). Confirming that $Pt(NO_2)_4^{2-}$ can itself relieve $Pt(NO_2)_4^{2-}$ block of F337A-CFTR, increasing the concentration of blocker from 100 to 300 μM during an individual experiment reduced current amplitude over most of the voltage range, but anomalously increased current amplitude below about −100 mV (Fig. 9, C–E). These current traces also suggest a possible explanation for this inverted concentration dependence. Relief of block by punchthrough is not apparent at 100 μM $Pt(NO_2)_4^{2-}$ (Fig. 9 D) or any concentration below this (unpublished data); however, punchthrough is clearly seen at 300 μM (Fig. 9 D) and 1 mM (Fig. 6). This suggests that the ability of $Pt(NO_2)_4^{2-}$ to permeate through the F337A channel pore is dependent on its own concentration. While we have not attempted to estimate the "permeability" of $Pt(NO_2)_4^{2-}$ in F337A-CFTR, we note

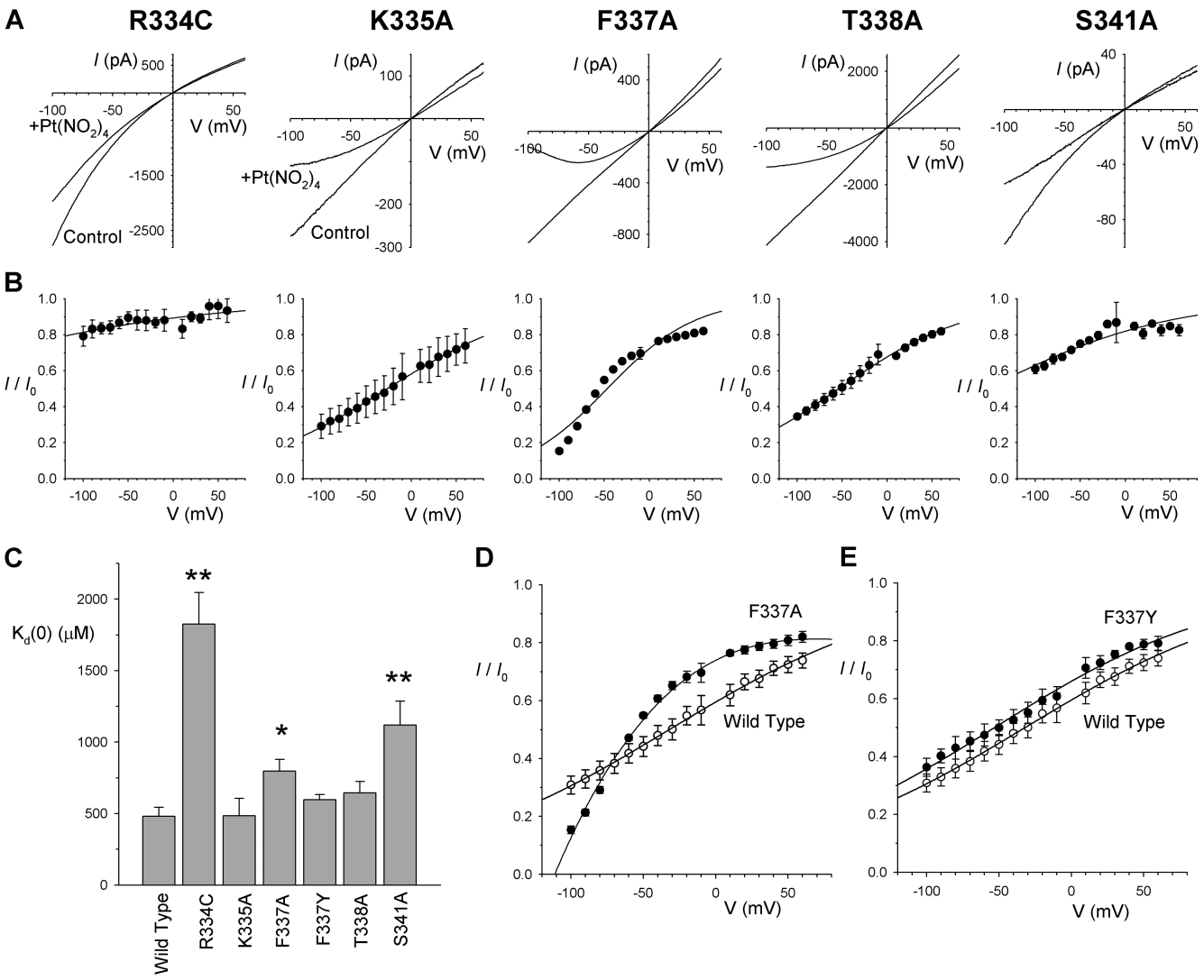

FIGURE 5. $Pt(NO_2)_4^{2-}$ block of TM6 mutant forms of CFTR. (A) Example macroscopic currents carried by the CFTR mutants R334C, K335A, F337A, T338A, and S341A before (Control) and after addition of 300 μM $Pt(NO_2)_4^{2-}$ to the intracellular solution. (B) Mean fraction of control current remaining following addition of this concentration of $Pt(NO_2)_4^{2-}$. Each plot has been fitted by Eq. 2; this provides a good fit of R334C ($K_d(0)$ = 2080 μM, $z\delta = -0.174$), K335A ($K_d(0)$ = 418 μM, $z\delta = -0.317$), T338A ($K_d(0)$ = 626 μM, $z\delta$ = –0.351) and S341A ($K_d(0)$ = 1362 μM, $z\delta$ = –0.249), but a poor fit of F337A. (C) Mean $K_d(0)$ estimated from fits such as those shown in B, except for F337A where $K_d(0)$ was calculated from the fractional current remaining (I/I_0) at 0 mV (estimated by fitting a polynomial function) according to the equation $K_d(0) = (I\,(300\ \mu M))/(I_0 - I)$. Asterisks signify a statistically significant difference from wild-type (*$P < 0.05$; **$P < 0.001$). (D) Comparison of the mean blocking effect of 300 μM intracellular $Pt(NO_2)_4^{2-}$ on wild-type (○; fitted by Eq. 2 as described in Fig. 2) and F337A (●; fitted by a third order polynomial function of no theoretical significance). (E) Comparison of the mean blocking effect of 300 μM intracellular $Pt(NO_2)_4^{2-}$ on wild-type (○; fitted as in D) and F337Y (●; fitted by Eq. 2 with $K_d(0)$ = 582 μM and $z\delta$ = –0.318). Mean of data from 4–9 patches in each of B–E.

that concentration-dependent ionic permeabilities are a well-known manifestation of anomalous mole fraction behavior (Hille, 2001).

The raw, unsubtracted current traces in Fig. 9 E show that the changes in current amplitude that underlie the negative slope conductance and apparent punchthrough observed during depolarizing voltage ramps occur over a slow timescale. To ensure that this did not, in fact, reflect time-dependent changes in F337A current amplitude, $Pt(NO_2)_4^{2-}$ block of F337A was also studied using a voltage-step protocol (Fig. 10). F337A-CFTR currents were practically time-independent in the absence and presence of $Pt(NO_2)_4^{2-}$ (Fig. 10 A). Confirming this, the voltage dependence of $Pt(NO_2)_4^{2-}$ block was similar to that observed with voltage ramps (Fig. 9 D), whether currents were measured early (100 ms; Fig. 10 B) or late (350 ms; Fig. 10 C) after the voltage step. The timecourse of $Pt(NO_2)_4^{2-}$ block was also confirmed using voltage steps to −150 mV (Fig. 11). Current amplitude

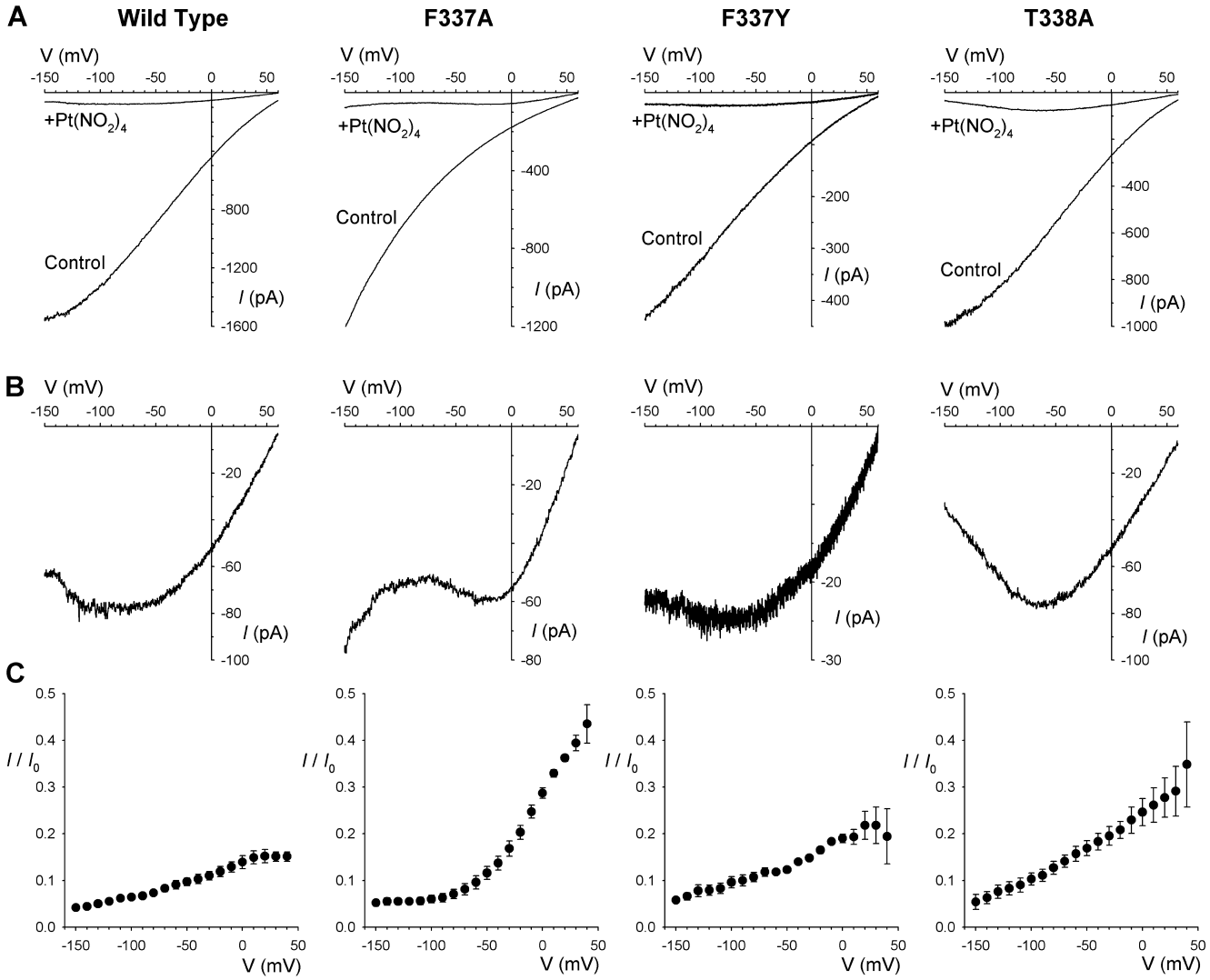

FIGURE 6. Apparent $Pt(NO_2)_4^{2-}$ unblock by permeation in F337A. (A) Example macroscopic currents carried by different CFTR variants before (Control) and after addition of 1 mM $Pt(NO_2)_4^{2-}$ to the intracellular solution at an extracellular Cl^- concentration of 4 mM. (B) Expanded current traces from A recorded in the presence of 1 mM $Pt(NO_2)_4^{2-}$. (C) Mean fraction of control current remaining following addition of 1 mM $Pt(NO_2)_4^{2-}$. Mean of data from 4–5 patches.

was effectively instantly affected by addition of $Pt(NO_2)_4^{2-}$ (Fig. 11 A).

Punchthrough of $Pt(NO_2)_4^{2-}$ in F337A was blocked by extracellular Cl^- ions (Fig. 7). As a result, block of this mutant by 300 μM $Pt(NO_2)_4^{2-}$ showed a complex dependence on external Cl^- concentration (Fig. 12). At positive voltages, $Pt(NO_2)_4^{2-}$ block was weakened by extracellular Cl^- (Fig. 12), as already shown for wild-type (Fig. 2 C); this effect, which is observed for many different CFTR open channel blockers, presumably reflects "knock off" of blocking $Pt(NO_2)_4^{2-}$ ions within the pore (McDonough et al., 1994; Linsdell et al., 1997; Zhou et al., 2002; Gong and Linsdell, 2003a). At very negative voltages, however, $Pt(NO_2)_4^{2-}$ block of F337A is anomalously strengthened by high extracellular Cl^- concentrations (Fig. 12). As described above, this block-enhancing effect of Cl^- ions appears to result from Cl^- preventing $Pt(NO_2)_4^{2-}$ from exiting the pore to the extracellular solution; this explanation is analogous to a "lock in" mechanism first described in Ca^{2+}-activated K^+ channels (Neyton and Miller, 1988a).

DISCUSSION

CFTR is potently inhibited by the highly permeant monovalent pseudohalide anion $Au(CN)_2^-$ (Linsdell and Gong, 2002). Under conditions similar to those used here (Fig. 1), we estimated a K_d at 0 mV of <200 μM for open channel block by intracellular $Au(CN)_2^-$ ions. Block is weaker for the divalent pseudohalides $Pt(NO_2)_4^{2-}$ (K_d 556 μM at 0 mV) and $PtCl_4^{2-}$ (K_d 969

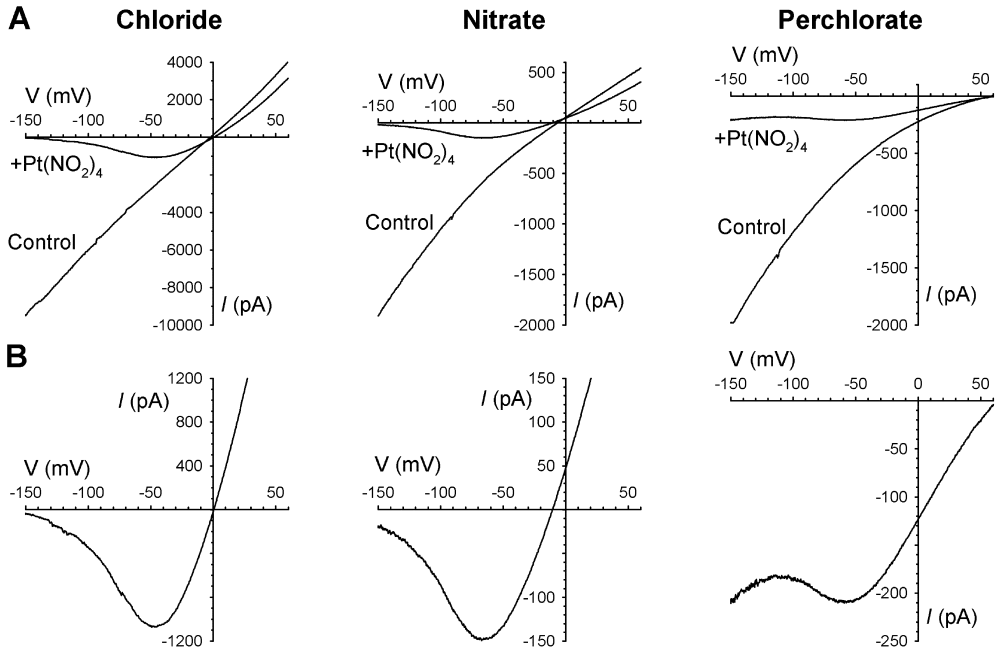

FIGURE 7. $Pt(NO_2)_4^{2-}$ punchthrough in F337A is prevented by extracellular permeant anions. (A) Example macroscopic currents carried by F337A-CFTR before (Control) and after addition of 1 mM $Pt(NO_2)_4^{2-}$ to the intracellular solution, with 150 mM chloride, nitrate or perchlorate present in the extracellular solution. (B) Expanded current traces from A recorded in the presence of 1 mM $Pt(NO_2)_4^{2-}$. Representative example traces of 3–5 patches showing the same effect in each case.

μM at 0 mV), while the trivalent anions $Fe(CN)_6^{3-}$ and $Co(CN)_6^{3-}$ appear ineffective as blockers (Fig. 1). Thus, based on this limited survey of pseudohalide anions, there appears to be a charge-dependent process excluding polyvalent anions from the CFTR pore.

$Pt(NO_2)_4^{2-}$ inhibits wild-type CFTR more potently from the intracellular than the extracellular solution (Fig. 3). When applied intracellularly, it blocks in a voltage-dependent manner (Fig. 1, A and C) by reducing apparent unitary current amplitude (Fig. 3, A and B). Block is strengthened by decreasing extracellular Cl^- concentration (Fig. 2 C) and weakened after mutagenesis of TM6 residues R334, F337, and S341 (Fig. 5). Thus, the inhibitory effects of $Pt(NO_2)_4^{2-}$ are similar to

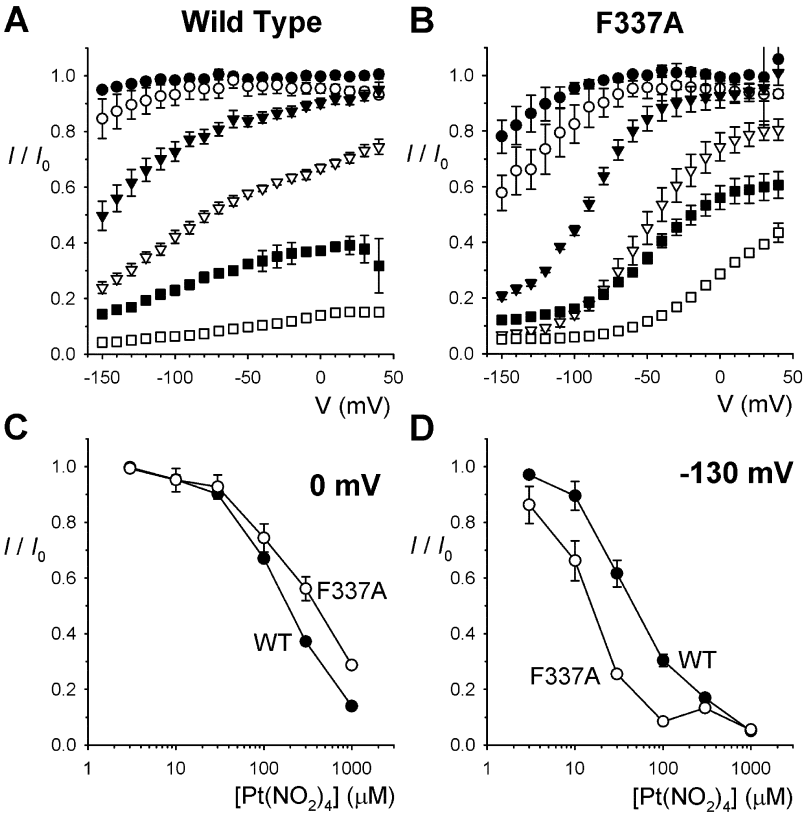

FIGURE 8. Comparison of the blocking effects of intracellular $Pt(NO_2)_4^{2-}$ on wild-type and F337A-CFTR at low extracellular Cl^- concentration. (A and B) Mean fraction of control current remaining following addition of 3 μM (●), 10 μM (○), 30 μM (▼), 100 μM (▽), 300 μM (■), or 1 mM (□) $Pt(NO_2)_4^{2-}$ to the intracellular solution, for wild-type (A) and F337A (B). (C and D) Comparison of the concentration dependence of block in wild-type (●) and F337A (○) at two different membrane potentials: 0 mV (C) and −130 mV (D). Mean of data from 3–4 patches in each case.

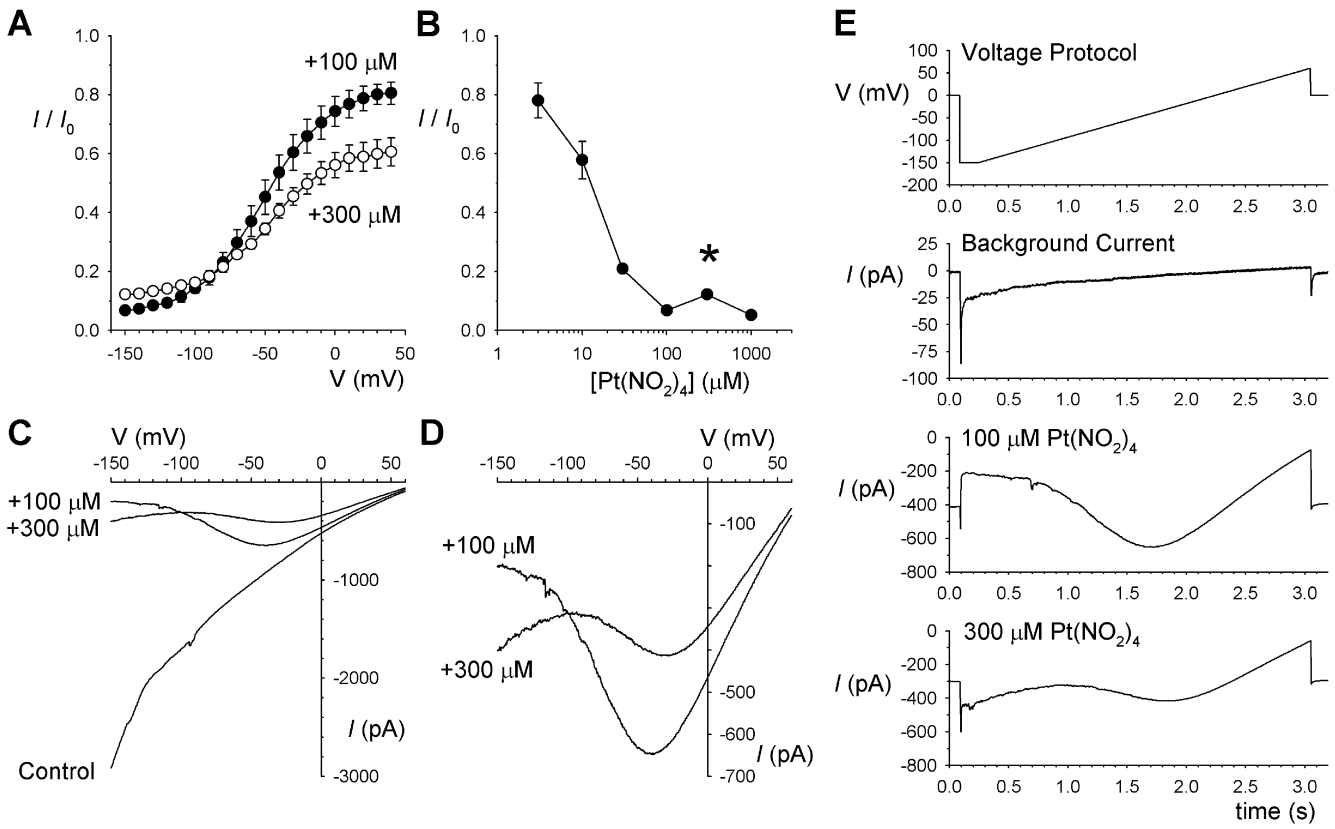

FIGURE 9. Increasing intracellular $Pt(NO_2)_4^{2-}$ concentration leads to weakening of block. (A) Mean fraction of control current remaining after addition of 100 μM (●) or 300 μM (○) $Pt(NO_2)_4^{2-}$ with 4 mM Cl^- in the extracellular solution. (B) Concentration dependence of block at −150 mV. The asterisk indicates a significant difference in fraction of control current remaining at 300 μM $Pt(NO_2)_4^{2-}$ from that at either 100 μM or 1 mM ($P < 0.001$). Mean of data from 3–5 patches in A and B. (C) Example macroscopic current recorded before addition of $Pt(NO_2)_4^{2-}$ (Control) and after sequential addition of $Pt(NO_2)_4^{2-}$ to final concentrations of 100 μM and 300 μM. Representative example of four patches showing the same effect. (D) Expanded current traces from C showing the complex effects of increasing $Pt(NO_2)_4^{2-}$ concentration; at membrane potential positive to −100 mV, block is strengthened as expected, whereas at more negative voltages block is anomalously weakened on addition of additional blocker. (E) Raw unsubtracted current traces from which the example in C and D is taken, showing the slow timescale of $Pt(NO_2)_4^{2-}$-induced changes in *I*V relationship shape. Note the different current scale of the background and stimulated current traces.

a broad range of other anions that act as open channel blockers of the CFTR pore (McDonough et al., 1994; Linsdell and Hanrahan, 1996a,b, 1999; Sheppard and Robinson, 1997; Hwang and Sheppard, 1999; Linsdell, 2001b; Gong et al., 2002b; Zhou et al., 2002). Indeed, it is not even a particularly potent open channel blocker (see above). Our interest in this substance stems from the consequences of a mutation within the pore (F337A) that apparently turns the channel from being $Pt(NO_2)_4^{2-}$ impermeable to $Pt(NO_2)_4^{2-}$ permeable (Fig. 6) and destroys the apparent simplicity of blocking effect seen in wild-type.

We found no evidence for $Pt(NO_2)_4^{2-}$ permeability in wild-type CFTR (Figs. 4 and 6), consistent with previous work (Smith and Dawson, 2001). However, punchthrough of $Pt(NO_2)_4^{2-}$ at negative voltages suggests that this anion is capable of passing through the pore of F337A-CFTR (Figs. 6, 7, and 9–11). As described by Nimigean and Miller (2002), the punchthrough phenomenon may be able to reveal very low levels of permeability inaccessible by other experimental means, and punchthrough of $Pt(NO_2)_4^{2-}$ was only observed under highly specific conditions (in F337A only, at voltages more negative than approximately −80 mV, low extracellular permeant anion concentration, and $Pt(NO_2)_4^{2-}$ concentrations of at least 300 μM). Nevertheless, the results shown in Fig. 6 suggest that the F337A mutation confers $Pt(NO_2)_4^{2-}$ permeability on the pore. Previously, we showed that the mutations F337A and F337S, but not F337Y, disrupted the ability of the CFTR channel pore to select between permeant anions on the basis of free energy of hydration (Linsdell et al., 2000) and suggested that F337 contributes to a lyotropic anion "selectivity filter." In contrast, mutations of the adjacent TM6 residue (T338), including T338A, altered the selectivity between different lyotro-

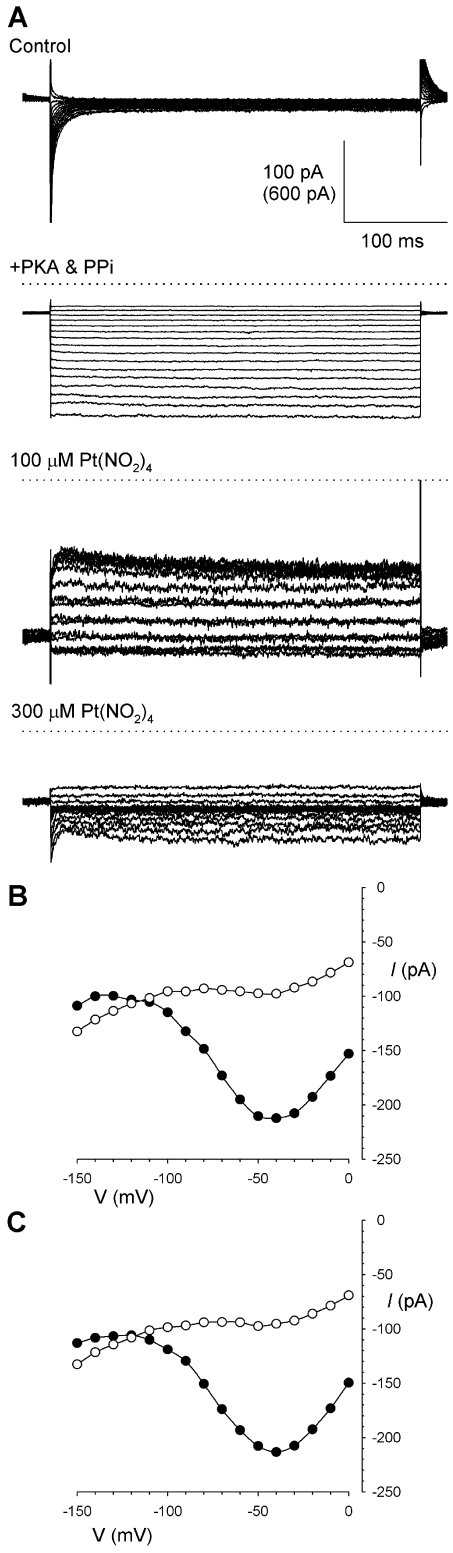

FIGURE 10. $Pt(NO_2)_4^{2-}$ block of F337A investigated using a voltage-step protocol. (A) Example F337A-CFTR currents in an inside-out patch, recorded before current activation (Control), after full current activation with PKA and PPi, and following sequential addition of $Pt(NO_2)_4^{2-}$ to final concentrations of 100 and 300 μM. Voltage steps were applied from a holding potential of −17 mV to test potentials between 0 and −150 mV in 10-mV increments. The current scale is 600 pA for the "+PKA & PPi" trace, and 100 pA for all others. Apart from the control traces themselves, all traces have had the control (leak) current digitally subtracted. Dotted lines represent the zero current level. Note that, for 100 μM $Pt(NO_2)_4^{2-}$, there is overlap between currents recorded at different voltages, due to the regions of negative conductance in the current-voltage relationship. (B and C) Current-voltage relationships from this patch in the presence of 100 μM (○) and 300 μM (●) $Pt(NO_2)_4^{2-}$, measured either 100 ms (B) or 350 ms (C) after the step change in voltage. Representative example traces of 4 patches showing the same effect.

pic anions but not that for lyotropes over kosmotropic anions (Linsdell et al., 1998). The slight $Pt(NO_2)_4^{2-}$ permeability of F337A therefore suggests that this divalent anion might normally be prevented from passing through the pore for similar reasons that limit the permeability of kosmotropic anions like F^-. In contrast, the T338A mutation appears to enhance unblock by permeation of the lyotropic $Au(CN)_2^-$ ion (Gong and Linsdell, 2003b). Previously, CFTR monovalent/divalent anion selectivity has been suggested to involve the TM6 residue S341 (McCarty and Zhang, 2001).

In addition to allowing $Pt(NO_2)_4^{2-}$ permeability, the F337A mutation has a complex effect on the apparent affinity of $Pt(NO_2)_4^{2-}$ block (Figs. 5 D and 8, B and D): block appears weaker than for wild-type at positive voltages yet stronger than in wild-type at negative voltages (and then weakens again in F337A due to punch-through; see below). The block observed in F337A is poorly fitted by conventional models that assume a single binding site (Fig. 5 B). We suggest that this reflects binding to more than one site in the F337A-CFTR pore; a low affinity site that is accessible at all voltages, and a higher affinity site that is increasingly accessed at more negative voltages. The existence of more than one $Pt(NO_2)_4^{2-}$ binding site in the F337A pore is also supported by the apparent anomalous mole fraction dependence of $Pt(NO_2)_4^{2-}$ permeability (Fig. 9). Since this complex blocking behavior is observed in F337A but not in wild-type or F337Y, we suggest that by allowing $Pt(NO_2)_4^{2-}$ to permeate through the pore, the F337A mutant also allows this blocker to reach a binding site which is normally inaccessible or much less easily accessed. We cannot rule out that $Pt(NO_2)_4^{2-}$ also acts at multiple sites in the wild-type pore.

A simple model of $Pt(NO_2)_4^{2-}$ movement in the F337A pore is shown in Fig. 13. Even in this mutant, $Pt(NO_2)_4^{2-}$ unblock by permeation only occurs under extreme conditions (strongly hyperpolarized voltages, low extracellular Cl^- concentrations, and high $Pt(NO_2)_4^{2-}$ concentration; Fig. 6), such that it appears that the blocker normally exits the F337A pore back into the intracellular solution. We therefore envision two barriers to $Pt(NO_2)_4^{2-}$ permeation in the pore; one between the two binding sites that may be more easily

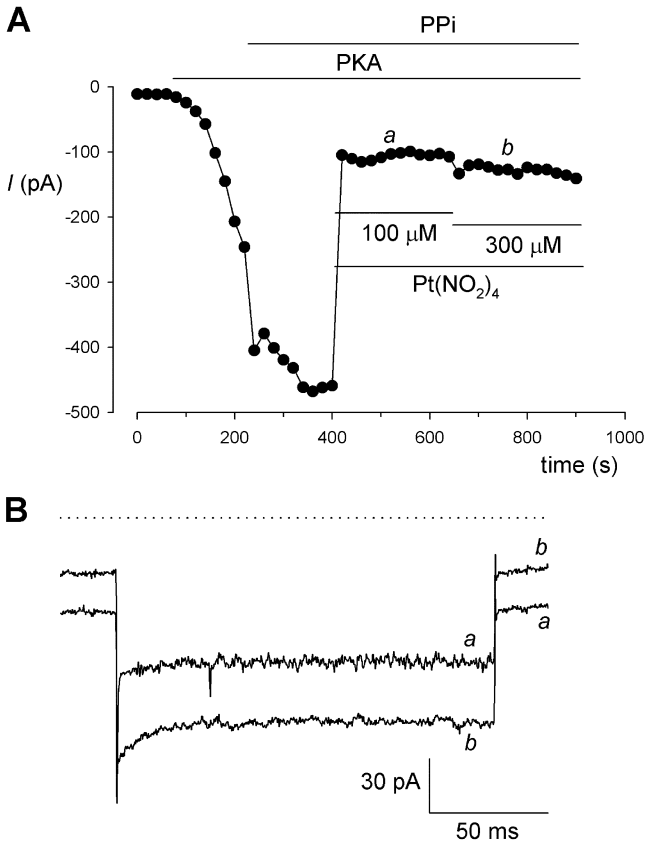

FIGURE 11. Timecourse of $Pt(NO_2)_4^{2-}$ block of F337A investigated using a voltage-step protocol. (A) Macroscopic current amplitude at −150 mV during sequential stimulation with PKA and PPi, and after sequential addition of $Pt(NO_2)_4^{2-}$ to final concentrations of 100 and 300 μM. Current at −150 mV is strongly blocked by 100 μM $Pt(NO_2)_4^{2-}$; however, block is immediately weakened on increasing the $Pt(NO_2)_4^{2-}$ concentration to 300 μM. (B) Example voltage steps (from a holding potential of −17 mV to a test potential of −150 mV) at the points indicated *a* and *b* in A. Consistent with the shape of the I-V relationships in Figs. 9 D and 10, B and C, the inward current at −17 mV is more strongly blocked by 300 μM $Pt(NO_2)_4^{2-}$, whereas the inward current at −150 mV is more strongly blocked by 100 μM $Pt(NO_2)_4^{2-}$. Dotted lines represent the zero current level. Representative example traces of three patches showing the same effect.

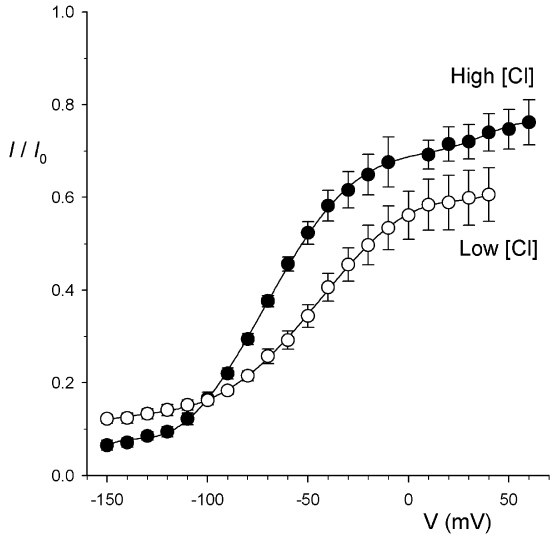

FIGURE 12. Complex effect of extracellular Cl^- concentration on block of F337A-CFTR by 300 μM $Pt(NO_2)_4^{2-}$. Mean fraction of control current remaining following addition of this concentration of $Pt(NO_2)_4^{2-}$ at high (154 mM; ●) and low (4 mM, Cl^- replaced by gluconate; ○) extracellular Cl^- concentration.

overcome in F337A than in wild-type, and a second barrier external to the outermost $Pt(NO_2)_4^{2-}$ binding site depicted in Fig. 13. In fact, the inability of $Pt(NO_2)_4^{2-}$ to pass easily between a high-affinity binding site and the extracellular solution is implied by the fact that $Pt(NO_2)_4^{2-}$ is a relatively weak blocker of wild-type CFTR when present in the extracellular solution (Fig. 3, C and D). With the addition of a second barrier to $Pt(NO_2)_4^{2-}$ movement in the pore (Fig. 13), our model appears able to explain the complex interaction between $Pt(NO_2)_4^{2-}$ and F337A-CFTR. At depolarized voltages, the blocker enters shallowly into the pore (Fig. 13 A), resulting in relatively weak block at these membrane potentials (Fig. 5 D). When the membrane is hyperpolarized, the blocker is driven further into the pore, where it encounters a higher affinity binding site (Fig. 13 B), resulting in a strong, highly voltage-dependent component of block (Fig. 5 D). The weak evidence supporting the existence of multiple anion binding sites in wild-type CFTR (such as the apparently concentration-dependent Hill coefficient; see Fig. 1, B and C) may in fact reflect a much lower, but nonzero, probability of $Pt(NO_2)_4^{2-}$ accessing this second site in the wild-type pore. At low concentrations of $Pt(NO_2)_4^{2-}$, the blocker returns from the high affinity site in F337A to the intracellular solution (Fig. 13 B). However, when the blocker concentration is increased to at least 300 μM, it is able to pass through the channel and so block is relieved by a punchthrough mechanism (Figs. 6 and 13 C). This apparent concentration-dependent $Pt(NO_2)_4^{2-}$ permeability is an unusually low concentration example of an anomalous mole fraction effect, usually ascribed to ion–ion interactions within multiion channel pores (Hille, 2001). Mechanistically, we suggest that at concentrations >300 μM, the F337A pore begins to show multiple occupancy by $Pt(NO_2)_4^{2-}$ ions, and that repulsion between simultaneously bound ions is capable of expelling ions bound to the "outer" site into the extracellular solution, relieving the high-affinity block (Fig. 13 C). This punchthrough of $Pt(NO_2)_4^{2-}$ is prevented by extracellular Cl^- or NO_3^- ions (Fig. 6), presumably by a "lock-in" effect (Fig. 13 D); Cl^- or NO_3^- binding in the outer mouth of the pore either physically or electrostatically prevents $Pt(NO_2)_4^{2-}$ from exiting the pore, and so even in multiply occupied

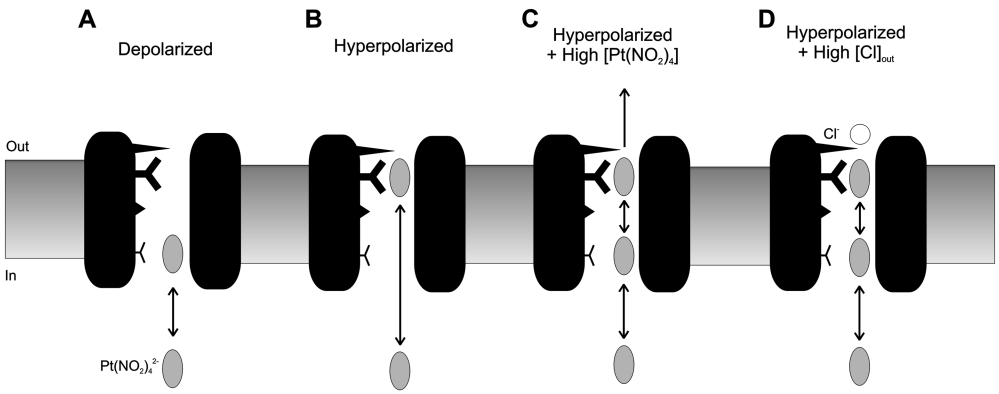

FIGURE 13. A pictorial model of $Pt(NO_2)_4^{2-}$ block in F337A-CFTR. $Pt(NO_2)_4^{2-}$ is assumed to have access to two distinct binding sites in the pore. (A) At depolarized voltages, $Pt(NO_2)_4^{2-}$ enters only shallowly into the pore, and block is weak. (B) At hyperpolarized voltages, $Pt(NO_2)_4^{2-}$ is driven deeper into the pore, where it interacts with a higher affinity binding site. (C) At high intracellular $Pt(NO_2)_4^{2-}$ concentrations, multiple occupancy allows $Pt(NO_2)_4^{2-}$ permeation through the pore as a result of destabilization between concurrently bound ions. (D) $Pt(NO_2)_4^{2-}$ permeation through the pore is blocked by extracellular Cl^- ions. Our experiments do not give any information as to the location of the extracellular Cl^- ion binding site underlying this effect, and a Cl^- ion is simply shown occluding the outer mouth of the pore. This effect of extracellular Cl^- is mimicked by the highly permeant NO_3^-, but not by the weakly permeant ClO_4^- or the impermeant gluconate.

channels the blocker molecules ultimately return to the intracellular solution. Interestingly, this lock-in effect of the permeant anions Cl^- and NO_3^- is apparently not shared by the impermeant kosmotropic anion gluconate (Fig. 6) or the weakly permeant lyotropic anion ClO_4^- (Fig. 7), even though ClO_4^- has been shown to bind tightly within the pore (Linsdell, 2001a). Thus, it appears that extracellular anions need to be permeant in order to lock intracellular $Pt(NO_2)_4^{2-}$ ions in the pore, perhaps reflecting that they must enter deeply into the pore from the extracellular solution to do so.

Previous evidence that CFTR has a multiion pore has come from anomalous mole fraction effects on anion unitary conductance (Tabcharani et al., 1993; but see Linsdell, 2001c) and from apparent interactions between permeant and blocking anions bound simultaneously within the pore (Zhou et al., 2002; Gong and Linsdell, 2003a). The present results suggest that multiple $Pt(NO_2)_4^{2-}$ ions can bind simultaneously within the F337A-CFTR pore (and perhaps also wild-type CFTR), and also that $Pt(NO_2)_4^{2-}$ binding may be able to occur concurrently with binding of extracellular Cl^- or NO_3^- ions. These results are therefore in agreement with previous results that permeant and blocking ions can bind simultaneously within the pore, and that the mutual destabilization associated with concurrent ion binding can speed anion exit from the pore (Zhou et al., 2002; Gong and Linsdell, 2003a). Furthermore, our results suggest that binding of multiple $Pt(NO_2)_4^{2-}$ anions inside the pore promotes their permeability through the pore, probably by a similar destabilizing effect. Whether multiple Cl^- ions bind within the pore during the normal permeation mechanism is much more difficult to prove (Dutzler et al., 2003).

Our results suggest that, by removing a barrier to $Pt(NO_2)_4^{2-}$ movement in the pore, the F337A mutation allows this anion to access a relatively high affinity binding site and simultaneously exposes it to multiion pore effects that destabilize its binding at high concentrations. This combination of tight binding and multiion destabilization leading to permeation has obvious parallels to the mechanism of cation permeation in voltage-gated K^+ and Ca^{2+} channels, where the permeant ion binds tightly within the selectivity filter region, and is then destabilized and caused to permeate by repulsive interactions with other ions entering this region (Bernèche and Roux, 2001; Morais-Cabral et al., 2001; Sather and McCleskey, 2003). Potentially a similar mechanism may be used to allow rapid Cl^- ion permeation in anion channel pores.

We thank Susan Burbridge for technical assistance, and Drs. Steve Barnes and John Hanrahan for comments on the manuscript.

This work was supported by the Canadian Institutes of Health Research and the Canadian Cystic Fibrosis Foundation (CCFF). X. Gong is a CCFF postdoctoral fellow. P. Linsdell is a CCFF scholar.

Olaf S. Andersen served as editor.

Submitted: 17 June 2003
Accepted: 7 October 2003

REFERENCES

Bähring, R., D. Bowie, M. Benveniste, and M.L. Mayer. 1997. Permeation and block of rat GluR6 glutamate receptor channels by internal and external polyamines. *J. Physiol.* 502:575–589.

Bernèche, S., and B. Roux. 2001. Energetics of ion conduction through the K^+ channel. *Nature.* 414:73–77.

Bormann, J., O.P. Hamill, and B. Sakmann. 1987. Mechanism of anion permeation through channels gated by glycine and γ-aminobutyric acid in mouse cultured spinal neurones. *J. Physiol.* 385: 243–286.

Dawson, D.C., S.S. Smith, and M.K. Mansoura. 1999. CFTR: mechanism of anion conduction. *Physiol. Rev.* 79:S47–S75.

Doyle, D.A., J.M. Cabral, R.A. Pfuetzner, A. Kuo, J.M. Gulbis, S.L.

Cohen, B.T. Chait, and R. MacKinnon. 1998. The structure of the potassium channel: molecular basis of K^+ conduction and selectivity. *Science.* 280:69–77.

Dutzler, R., E.B. Campbell, M. Cadene, B.T. Chait, and R. MacKinnon. 2002. X-ray structure of a ClC chloride channel at 3.0 Å reveals the molecular basis of anion selectivity. *Nature.* 415:287–294.

Dutzler, R., E.B. Campbell, and R. MacKinnon. 2003. Gating the selectivity filter in ClC chloride channels. *Science.* 300:108–112.

Fahlke, C., C. Dürr, and A.L. George. 1997. Mechanism of ion permeation in skeletal muscle chloride channels. *J. Gen. Physiol.* 110: 551–564.

French, R.J., and J.J. Shoukimas. 1985. An ion's view of the potassium channel. The structure of the permeation pathway as sensed by a variety of blocking ions. *J. Gen. Physiol.* 85:669–698.

French, R.J., and J.B. Wells. 1977. Sodium ions as blocking agents and charge carriers in the potassium channel of the squid giant axon. *J. Gen. Physiol.* 70:707–724.

Gong, X., and P. Linsdell. 2003a. Coupled movement of permeant and blocking ions in the CFTR chloride channel pore. *J. Physiol.* 549:375–385.

Gong, X., and P. Linsdell. 2003b. Molecular determinants and role of an anion binding site in the external mouth of the CFTR chloride channel pore. *J. Physiol.* 549:387–397.

Gong, X., S.M. Burbridge, E.A. Cowley, and P. Linsdell. 2002a. Molecular determinants of $Au(CN)_2^-$ binding and permeability within the cystic fibrosis transmembrane conductance regulator Cl^- channel pore. *J. Physiol.* 540:39–47.

Gong, X., S.M. Burbridge, A.C. Lewis, P.Y.D. Wong, and P. Linsdell. 2002b. Mechanism of lonidamine inhibition of the CFTR chloride channel. *Br. J. Pharmacol.* 137:928–936.

Gunderson, K.L., and R.R. Kopito. 1994. Effects of pyrophosphate and nucleotide analogs suggest a role for ATP hydrolysis in cystic fibrosis transmembrane regulator channel gating. *J. Biol. Chem.* 269:19349–19353.

Gunderson, K.L., and R.R. Kopito. 1995. Conformational states of CFTR associated with channel gating: the role of ATP binding and hydrolysis. *Cell.* 82:231–239.

Gupta, J., and P. Linsdell. 2002. Point mutations in the pore region directly or indirectly affect glibenclamide block of the CFTR chloride channel. *Pflugers Arch.* 443:739–747.

Gupta, J., and P. Linsdell. 2003. Extent of the selectivity filter region in the CFTR chloride channel. *Mol. Membr. Biol.* 20:45–52.

Halm, D.R., and R.A. Frizzell. 1992. Anion permeation in an apical membrane chloride channel of a secretory epithelial cell. *J. Gen. Physiol.* 99:339–366.

Hebeisen, S., H. Heidtmann, D. Cosmelli, C. Gonzalez, B. Poser, R. Latorre, O. Alvarez, and C. Fahlke. 2003. Anion permeation in human ClC-4 channels. *Biophys. J.* 84:2306–2318.

Hille, B. 2001. Ion Channels of Excitable Membranes. 3rd ed. Sinauer Associates, Inc., Sunderland, MA. 814 pp.

Hodgkin, A.L., and R.D. Keynes. 1955. The potassium permeability of a giant nerve fibre. *J. Physiol.* 128:61–88.

Huang, C.-J., and E. Moczydlowski. 2001. Cytoplasmic polyamines as permeant blockers and modulators of the voltage-gated sodium channel. *Biophys. J.* 80:1262–1279.

Huang, C.-J., I. Favre, and E. Moczydlowski. 2000. Permeation of large tetra-alkylammonium cations through mutant and wild-type voltage-gated sodium channels as revealed by relief of block at high voltage. *J. Gen. Physiol.* 115:435–453.

Hwang, T.-C., and D.N. Sheppard. 1999. Molecular pharmacology of the CFTR Cl^- channel. *Trends Pharmacol. Sci.* 20:448–453.

Jiang, Y., and R. MacKinnon. 2000. The barium site in a potassium channel by X-ray crystallography. *J. Gen. Physiol.* 115:269–272.

Kerschbaum, H.H., J.A. Kozak, and M.D. Cahalan. 2003. Polyvalent cations as permeant probes of MIC and TRPM7 pores. *Biophys. J.* 84:2293–2305.

Linsdell, P. 2001a. Relationship between anion binding and anion permeability revealed by mutagenesis within the cystic fibrosis transmembrane conductance regulator chloride channel pore. *J. Physiol.* 531:51–66.

Linsdell, P. 2001b. Direct block of the cystic fibrosis transmembrane conductance regulator Cl^- channel by butyrate and phenylbutyrate. *Eur. J. Pharmacol.* 411:255–260.

Linsdell, P. 2001c. Thiocyanate as a probe of the cystic fibrosis transmembrane conductance regulator chloride channel pore. *Can. J. Physiol. Pharmacol.* 79:573–579.

Linsdell, P., and X. Gong. 2002. Multiple inhibitory effects of $Au(CN)_2^-$ ions on cystic fibrosis transmembrane conductance regulator Cl^- channel currents. *J. Physiol.* 540:29–38.

Linsdell, P., and J.W. Hanrahan. 1996a. Disulphonic stilbene block of cystic fibrosis transmembrane conductance regulator Cl^- channels expressed in a mammalian cell line and its regulation by a critical pore residue. *J. Physiol.* 496:687–693.

Linsdell, P., and J.W. Hanrahan. 1996b. Flickery block of single CFTR chloride channels by intracellular anions and osmolytes. *Am. J. Physiol.* 271:C628–C634.

Linsdell, P., and J.W. Hanrahan. 1998. Adenosine triphosphate-dependent asymmetry of anion permeation in the cystic fibrosis transmembrane conductance regulator chloride channel. *J. Gen. Physiol.* 111:601–614.

Linsdell, P., and J.W. Hanrahan. 1999. Substrates of multidrug resistance-associated proteins block the cystic fibrosis transmembrane conductance regulator chloride channel. *Br. J. Pharmacol.* 126: 1471–1477.

Linsdell, P., A. Evagelidis, and J.W. Hanrahan. 2000. Molecular determinants of anion selectivity in the cystic fibrosis transmembrane conductance regulator chloride channel pore. *Biophys. J.* 78:2973–2982.

Linsdell, P., J.A. Tabcharani, and J.W. Hanrahan. 1997. Multi-ion mechanism for ion permeation and block in the cystic fibrosis transmembrane conductance regulator chloride channel. *J. Gen. Physiol.* 110:365–377.

Linsdell, P., S.-X. Zheng, and J.W. Hanrahan. 1998. Non-pore lining amino acid side chains influence anion selectivity of the human CFTR Cl^- channel expressed in mammalian cell lines. *J. Physiol.* 512:1–16.

McCarty, N.A., and Z.-R. Zhang. 2001. Identification of a region of strong discrimination in the pore of CFTR. *Am. J. Physiol. Lung Cell Mol Physiol.* 281:L852–L867.

McDonough, S., N. Davisdon, H.A. Lester, and N.A. McCarty. 1994. Novel pore-lining residues in CFTR that govern permeation and open-channel block. *Neuron.* 13:623–634.

Morais-Cabral, J.H., Y. Zhou, and R. MacKinnon. 2001. Energetic optimization of ion conduction rate by the K^+ selectivity filter. *Nature.* 414:37–42.

Neyton, J., and C. Miller. 1988a. Potassium blocks barium permeation through a calcium-activated potassium channel. *J. Gen. Physiol.* 92:549–567.

Neyton, J., and C. Miller. 1988b. Discrete Ba^{2+} block as a probe of ion occupancy and pore structure in the high-conductance Ca^{2+}-activated K^+ channel. *J. Gen. Physiol.* 92:569–586.

Nimigean, C.M., and C. Miller. 2002. Na^+ block and permeation in a K^+ channel of known structure. *J. Gen. Physiol.* 120:323–335.

Pusch, M., U. Ludewig, A. Rehfeldt, and T.J. Jentsch. 1995. Gating of the voltage-dependent chloride channel ClC-0 by the permeant anion. *Nature.* 373:527–531.

Qu, Z., and H.C. Hartzell. 2000. Anion permeation in Ca^{2+}-activated Cl^- channels. *J. Gen. Physiol.* 116:825–844.

Rychkov, G.Y., M. Pusch, M.L. Roberts, T.J. Jentsch, and A.H.

Bretag. 1998. Permeation and block of the skeletal muscle chloride channel, ClC-1, by foreign anions. *J. Gen. Physiol.* 111:653–665.

Sather, W.A., and E.W. McCleskey. 2003. Permeation and selectivity in calcium channels. *Annu. Rev. Physiol.* 65:133–159.

Sheppard, D.N., and K.A. Robinson. 1997. Mechanism of glibenclamide inhibition of cystic fibrosis transmembrane conductance regulator Cl^- channels expressed in a murine cell line. *J. Physiol.* 503:333–346.

Sheppard, D.N., and M.J. Welsh. 1999. Structure and function of the CFTR chloride channel. *Physiol. Rev.* 79:S23–S45.

Smith, S.S., and D.C. Dawson. 2001. CFTR: voltage-dependent block by divalent pseudohalides. *Biophys. J.* 80:469a.

Smith, S.S., E.D. Steinle, M.E. Meyerhoff, and D.C. Dawson. 1999. Cystic fibrosis transmembrane conductance regulator. Physical basis for lyotropic anion selectivity patterns. *J. Gen. Physiol.* 114: 799–818.

Tabcharani, J.A., X.-B. Chang, J.R. Riordan, and J.W. Hanrahan. 1991. Phosphorylation-regulated Cl^- channel in CHO cells stably expressing the cystic fibrosis gene. *Nature.* 352:628–631.

Tabcharani, J.A., J.M. Rommens, Y.-X. Hou, X.-B. Chang, L.-C. Tsui, J.R. Riordan, and J.W. Hanrahan. 1993. Multi-ion pore behaviour in the CFTR chloride channel. *Nature.* 366:79–82.

Walsh, K.B., K.J. Long, and X. Shen. 1999. Structural and ionic determinants of 5-nitro-2-(3-phenylpropyl-amino)-benzoic acid block of the CFTR chloride channel. *Br. J. Pharmacol.* 127:369–376.

Winters, C.J., and T.E. Andreoli. 2002. Cl^- channels in basolateral TAL membranes. XVII. Kinetic properties of mcClC-Ka, a basolateral CTAL Cl^- channel. *J. Membr. Biol.* 186:159–164.

Woodhull, A.M. 1973. Ionic blockage of sodium channels in nerve. *J. Gen. Physiol.* 61:687–708.

Zhang, Z.-R., S. Zeltwanger, and N.A. McCarty. 2000. Direct comparison of NPPB and DPC as probes of CFTR expressed in *Xenopus* oocytes. *J. Membr. Biol.* 175:35–52.

Zhou, Y., J.H. Morais-Cabral, A. Kaufman, and R. MacKinnon. 2001. Chemistry of ion coordination and hydration revealed by a K^+ channel-Fab complex at 2.0 Å resolution. *Nature.* 414:43–48.

Zhou, Z., S. Hu, and T.-C. Hwang. 2002. Probing an open CFTR pore with organic anion blockers. *J. Gen. Physiol.* 120:647–662.